COMPARATIVE ACCURACY ASSESSMENT OF UAV-DERIVED ORTHOPHOTO, DSM, AND DTM GENERATED WITH AND WITHOUT GROUND CONTROL POINTS: A CASE STUDY OF THE LMTC PREMISES, NEPAL

Bhuwan Singh Bisht [1], Nabaraj Subedi [1], Ram Kumar Sapkota [1], Laxmi Devi Thapa [1]
[1] *Land Management Training Center, Dhulikhel, Kavrepalanchok, Nepal*
geo.bhuwan@gmail.com ; nabaraj.ge@gmail.com ; ramksap1@gmail.com; thapalaxmi8182@gmail.com

KEY WORDS: UAV photogrammetry, ground control points (GCPs), checkpoints (CPs), orthophoto, digital surface model (DSM), digital terrain model (DTM), accuracy assessment

ABSTRACT:

Unmanned Aerial Vehicle (UAV) photogrammetry is increasingly used for local-scale mapping because it enables rapid generation of high-resolution orthophotos and elevation products. However, the positional and vertical quality of these products depends strongly on the georeferencing strategy, particularly the use of Ground Control Points (GCPs). This study evaluates the effect of GCPs on the accuracy of UAV-derived orthophoto, Digital Surface Model (DSM), and Digital Terrain Model (DTM) at the premises of the Land Management Training Center (LMTC), Dhulikhel, Nepal. The same UAV image block of 334 images was processed under two workflows: one using only onboard image geolocation and another using five surveyed GCPs. Eight independent checkpoints were used for accuracy assessment. Orthophoto planimetric accuracy was evaluated using checkpoint coordinates, while vertical agreement of DSM and DTM was assessed using surveyed ground elevations. In addition, pairwise checkpoint-distance analysis and supplementary object-based comparison were used to examine relative geometric differences in the orthophotos. The with-GCP orthophoto achieved a horizontal $RMSE_H$ of 0.063 m, whereas the without-GCP orthophoto showed an $RMSE_H$ of 3.507 m. Similarly, the with-GCP DSM and DTM achieved $RMSE_Z$ values of 0.131 m and 0.143 m, respectively, compared with 15.385 m and 15.347 m in the without-GCP workflow. The without-GCP orthophoto also exhibited systematic westward and northward displacement and minor scale-related geometric differences. The results demonstrate that GCP-based processing remains essential for reliable campus-scale UAV photogrammetry when the outputs are intended for measurement, terrain representation, planning, and other applications requiring dependable absolute accuracy.

1. INTRODUCTION

Unmanned Aerial Vehicle (UAV) photogrammetry has emerged as an efficient and accessible approach for generating high-resolution geospatial products for local-scale mapping and analysis. By acquiring multiple overlapping images from low-altitude aerial platforms and processing them through image matching, bundle adjustment, and three-dimensional reconstruction, UAV systems can produce orthophotos, Digital Surface Models (DSMs), and Digital Terrain Models (DTMs) suitable for surveying, engineering mapping, terrain analysis, infrastructure inspection, environmental monitoring, and land-management applications (Kovanič et al., 2023; Manfreda et al., 2018). Because UAV platforms are flexible, rapid, and comparatively low-cost, they are now widely used in site-scale geospatial workflows where timely and detailed spatial products are required.

The photogrammetric outputs derived from UAV imagery are fundamentally dependent on image geometry, flight configuration, and georeferencing quality. An orthophoto is a geometrically corrected aerial image in which relief and perspective distortions have been removed so that the image can be used for planimetric measurement. A DSM represents the elevation of the upper visible surface, including terrain, buildings, vegetation, and other above-ground objects, whereas a DTM represents the bare-earth terrain surface after excluding such features (Guth et al., 2021; Pix4D, n.d.-a). These products are valuable for mapping, planning, monitoring, and quantitative measurement, but their usefulness depends strongly on the positional and vertical reliability achieved during data acquisition and processing.

Previous studies have shown that the quality of UAV-derived products is influenced by several interacting factors, including flight altitude, image overlap, ground sampling distance, terrain complexity, camera calibration, flight geometry, and the software used for photogrammetric reconstruction (Gerke & Przybilla, 2016; Kovanič et al., 2023; Szypuła, 2024). Among these factors, georeferencing strategy plays a particularly important role in determining absolute positional accuracy. In practical UAV photogrammetry, Ground Control Points (GCPs) provide external geometric control by linking the image block to accurately surveyed ground coordinates, whereas checkpoints are reserved for independent validation and should not be used during model adjustment (Pix4D, n.d.-b; Sanz-Ablanedo et al., 2018). The number, spatial distribution, and quality of GCPs can substantially influence the final positional and vertical accuracy of orthophotos and elevation models (Martínez-Carricondo et al., 2018; Sanz-Ablanedo et al., 2018; Szypuła, 2024).

The need to compare with-GCP and without-GCP workflows is both technically and practically important. In many campus-scale and institutional UAV surveys, especially those carried out with consumer-grade platforms, there is often a tendency to rely only on onboard image geolocation in order to reduce field effort, time, and equipment requirements. However, several studies have shown that products generated without GCPs may appear visually coherent while still exhibiting weak absolute positional reliability (Szypuła, 2024; Žabota et al., 2021). This distinction is important because a product that appears visually acceptable may still be unsuitable for precise mapping, engineering measurement, or land-management applications that require dependable absolute positioning.

This issue is directly relevant to the premises of the Land Management Training Center (LMTC), Dhulikhel, Kavrepalanchok, Nepal, where the study area includes open ground, buildings, internal roads, and mixed surface conditions that are suitable for evaluating both planimetric and elevation products. In the present study, the same UAV image block was processed under two separate workflows: one using only onboard image geolocation and another using surveyed Ground Control Points. This design allows the effect of georeferencing strategy to be examined while keeping the study area, image dataset, and processing environment constant.

Accordingly, this study aims to assess the effect of Ground Control Points on the positional and elevation accuracy of UAV-derived orthophoto, DSM, and DTM products at the LMTC premises, Nepal. More specifically, the study compares with-GCP and without-GCP processing workflows, evaluates orthophoto planimetric accuracy using independent checkpoints, and assesses vertical agreement of the elevation products at surveyed ground checkpoint locations. In addition, the study examines whether the without-GCP orthophoto is affected only by systematic positional shift or also by relative geometric differences.

2. MATERIALS AND METHODS

2.1 Study area

The study was carried out within the premises of the Land Management Training Center (LMTC), located in Dhulikhel, Kavrepalanchok, Nepal, as shown in Figure 1. The study area covers 31,666.47 m² (approximately 3.17 ha).

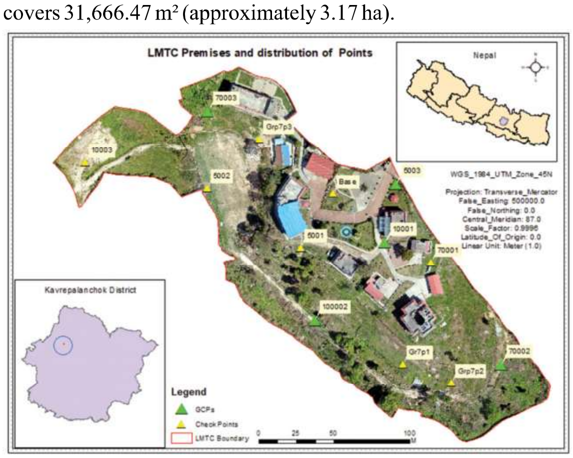

Figure 1. Location of the study area and distribution of Ground Control Points and checkpoints

2.2 Methodology

The overall methodology adopted in this study is illustrated in Figure 2. The workflow began with UAV data acquisition over the LMTC premises, followed by DGPS survey of pre-marked ground targets. The same UAV image block was then processed under two separate photogrammetric workflows: one using only onboard image geolocation and another using surveyed Ground Control Points (GCPs). In the with-GCP workflow, the surveyed GCPs were used for georeferencing, while the independent checkpoints were reserved only for validation. In the without-GCP workflow, no surveyed GCPs were introduced during processing, and georeferencing relied solely on onboard image geolocation.

After photogrammetric processing, the generated orthophoto, DSM, and DTM products from both workflows were clipped to the LMTC boundary in order to maintain a common analysis extent. Coordinates and elevation values were then extracted at the independent checkpoint locations for comparative evaluation. The resulting products were assessed through planimetric analysis of the orthophoto and vertical agreement assessment of the elevation products at the checkpoint locations. In addition, supplementary relative-geometry analysis was carried out to examine whether the without-GCP orthophoto was affected only by positional shift or also by scale-related geometric differences. The complete methodological sequence is presented in Figure 2.

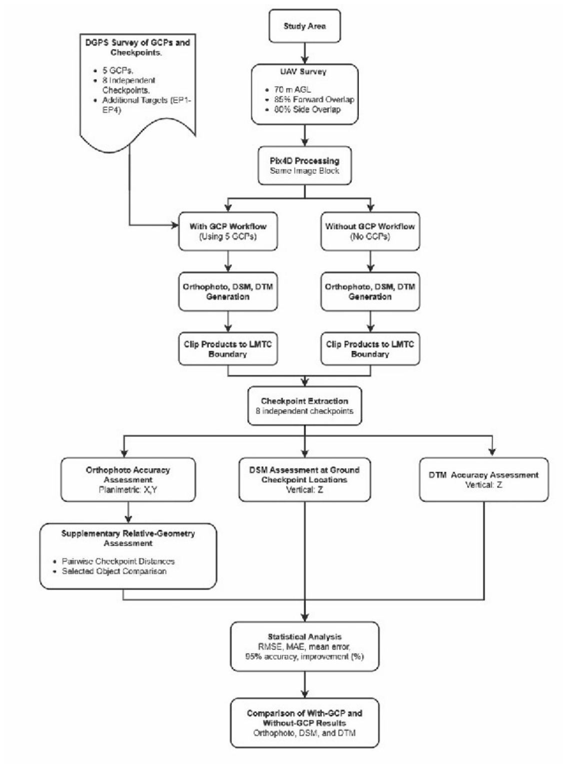

Figure 2. Methodological workflow of the study

2.3 UAV data acquisition

A UAV survey was conducted over the LMTC premises using a DJI Mavic 3 equipped with an RGB camera. Nadir images were acquired during the flight through the survey configuration. The flight was carried out at 70 m above ground level, maintaining 85% forward overlap and 80% side overlap. A total of 334 images were captured during the survey. These images were used to generate orthophoto, DSM, and DTM products under both processing scenarios.

2.4 Ground Control Points, Checkpoints, and Additional Targets

Pre-marked targets were established across the study area and surveyed on the ground using Trimble DGPS. Each station was observed for more than 2 hours, and the collected data were subsequently processed in Trimble Business Center software to obtain the final coordinates. The surveyed Ground Control Points (GCPs) and independent checkpoints listed in Table 1 are reported in the WGS 1984 UTM Zone 45N coordinate reference system (EPSG:32645). The projection is based on the Transverse Mercator system, with a central meridian of 87°, a scale factor of 0.9996, a false easting of 500000.0 m, and a false northing of 0.0 m. The horizontal coordinates are expressed in meters.

Because the study area was relatively small and campus-scale in extent, five GCPs were considered practically sufficient for external control in the present comparison. However, a denser and more widely distributed GCP network would provide stronger redundancy and may further improve georeferencing robustness in future studies.

Five points, GCP1, GCP2, GCP3, GCP4, and GCP5, were used as Ground Control Points in the with-GCP workflow, as shown in Table 1. These points were introduced during photogrammetric adjustment to constrain the model in the output coordinate system. Eight points, CP1 to CP8, were used as independent checkpoints and were excluded from the adjustment. After product generation, the same checkpoints were used to assess the accuracy of the orthophoto, DSM, and DTM by comparing the extracted coordinates and elevations with the surveyed values.

Table 1. Surveyed GCPs and checkpoints used in the study

SN	Point Name	Easting(m)	Northing(m)	Elevation(m)	Remarks
1	CP1	356092.046	3055879.615	1486.559	CP
2	CP2	356178.297	3055869.848	1483.357	CP
3	CP3	356113.241	3055915.189	1490.748	CP
4	CP4	356159.554	3055802.329	1480.710	CP
5	CP5	356191.748	3055790.117	1479.035	CP
6	CP6	356064.682	3055951.382	1482.868	CP
7	CP7	355949.173	3055935.794	1478.221	CP
8	CP8	356030.024	3055918.795	1478.808	CP
9	GCP1	356154.897	3055921.294	1489.883	GCP
10	GCP2	356147.720	3055882.701	1488.432	GCP
11	GCP3	356224.548	3055801.769	1475.884	GCP
12	GCP4	356030.447	3055969.268	1482.351	GCP
13	GCP5	356101.087	3055830.983	1475.703	GCP

In addition, four extra pre-marked targets, EP1 to EP4, were visible in the UAV products but were not surveyed in the field. Because their ground coordinates were not available, these points were not included in the quantitative accuracy assessment. However, they were used for supplementary visual and relative comparison between the with-GCP and without-GCP orthophotos. The classification of points used in the study is presented in Table 2.

Table 2. Point categories used in the study

Point category	Point IDs	Count	Use in analysis
Ground Control Points	GCP1, GCP2, GCP3, GCP4, GCP5	5	Georeferencing only
Independent checkpoints	CP1, CP2, CP3, CP4, CP5, CP6, CP7, CP8	8	Absolute accuracy assessment
Supplementary visual targets	EP1, EP2, EP3, EP4	4	Relative orthophoto shift only

2.5 Processing scenarios

The same UAV image block was processed under two separate workflows to evaluate the effect of georeferencing strategy on the final products. In the first workflow, the imagery was processed using only the onboard image geolocation recorded in the image metadata, and no surveyed control points were introduced during adjustment. In the second workflow, the same imagery was processed again using the five surveyed Ground Control Points as GCPs, while the eight independent checkpoints were assigned only as checkpoints for validation. After GCP marking, checkpoint assignment, and bundle adjustment, orthophoto, DSM, and DTM products were generated. Because the same image block and acquisition conditions were used in both cases, the comparison isolates the effect of GCP-based georeferencing on product accuracy.

The DTM used in this study was generated using the built-in terrain-model generation workflow in Pix4D Mapper. This clarification is important because DTM quality is dependent on the terrain-model generation and ground-classification procedure.

Pix4D Mapper was selected because it provides an integrated environment for image alignment, bundle adjustment, control-point management, orthophoto generation, DSM/DTM production, and processing-quality reporting within a single software workflow. Since the main objective of the study was to compare the effect of with-GCP and without-GCP georeferencing using the same UAV image block, the same processing software was intentionally retained for both workflows. A cross-software comparison could be valuable in future research, but it was beyond the scope of the present study.

1.2 Photogrammetric processing quality

The Pix4D quality reports indicate that both workflows calibrated all 334 images successfully. In the with-GCP workflow, the average GSD was 3.10 cm, the median number of keypoints per image was 11,242, the median number of matches per calibrated image was 6417.33, and the mean reprojection error was 0.146 pixel. Georeferencing was based on five 3D GCPs, with a mean RMS georeferencing error of 0.018 m. In the without-GCP workflow, the average GSD was 3.12 cm, the median number of keypoints per image was also 11,242, the median number of matches per calibrated image were 6422.72, and the mean reprojection error was 0.144 pixel. However, this workflow was processed without any 3D GCPs, and the camera optimization difference was noticeably larger, at 17.67%, than in the with-GCP workflow, where it was 3.65%. This indicates weaker geometric constraint in the no-control case. Selected processing-quality indicators derived from the Pix4D quality reports are summarised in Table 3.

Table 3. Selected processing-quality indicators from the Pix4D quality reports for the two workflows

Indicator	With GCP	Without GCP
Images calibrated	334/334	334/334
Average GSD	3.10 cm	3.12 cm
Median keypoints per image	11,242	11,242
Median matches per calibrated image	6417.330	6422.720
Mean reprojection error	0.146 pixel	0.144 pixel
Camera optimization difference	3.65%	17.67%
Georeferencing status	5 GCPs (5 3D), mean RMS 0.018 m	No 3D GCP

Further details from the Pix4D geolocation report of the with-GCP workflow showed that the GCP-based adjustment was well constrained. The GCP RMSE values were 0.022 m in X, 0.023 m in Y, and 0.010 m in Z, indicating a strong georeferencing fit. Independent checkpoint validation yielded RMSE values of 0.011 m in X, 0.031 m in Y, and 0.124 m in Z, demonstrating very good horizontal agreement and satisfactory vertical consistency. The absolute geolocation variance further indicated that the initial onboard image geolocation contained systematic offsets, with mean values of −1.478 m in X, 3.254 m in Y, and −0.867 m in Z. The corresponding RMS values were 1.496 m, 4.035 m, and 0.994 m, respectively. These results suggest that although the onboard image geotags provided a usable initial position, the incorporation of surveyed GCPs was essential for achieving reliable absolute georeferencing. The georeferencing and checkpoint statistics derived from the Pix4D geolocation report are presented in Table 4.

Table 4. Georeferencing and checkpoint accuracy statistics from the Pix4D geolocation report for the with-GCP workflow

Statistic	X (m)	Y (m)	Z (m)
GCP RMSE	0.022	0.023	0.01
Checkpoint RMSE	0.011	0.031	0.124
Mean absolute geolocation variance	-1.478	3.254	-0.867
RMS absolute geolocation variance	1.496	4.035	0.994

The GCP RMSE values represent the fit of surveyed ground control points after bundle adjustment. The checkpoint RMSE values represent independent validation accuracy. The absolute geolocation variance describes the difference between the initial onboard image geolocation and the adjusted image geolocation.

2.7 Accuracy assessment and statistical analysis

Accuracy assessment was carried out separately for the orthophoto and the elevation products generated under the with-GCP and without-GCP workflows. For the orthophoto, the surveyed coordinates of the independent checkpoints were compared with the corresponding coordinates extracted from the orthophoto to evaluate planimetric accuracy. For the elevation products, the surveyed elevations of the checkpoints were compared with the raster-derived elevation values extracted from the respective products to evaluate vertical agreement.

Because all vertical validation checkpoints used in this study were located on ground surfaces, the checkpoint-based vertical assessment primarily represents elevation agreement at ground locations. In this context, the DTM evaluation directly represents bare-earth agreement, whereas the DSM evaluation reflects raster elevation agreement at the same ground checkpoint locations only and does not provide validation of elevated surface features such as rooftops, vegetation canopies, or other above-ground objects.

Residuals were computed as the differences between the model-derived values and the surveyed reference values. The residuals in the X and Y directions express planimetric displacement in easting and northing, respectively, while the residual in the Z direction expresses vertical deviation. For the orthophoto, these two horizontal residual components were combined into a single radial planimetric error term. For the elevation products, the vertical residual directly represents the difference between the extracted raster elevation and the surveyed elevation. The accuracy assessment in this study was based on eight independent checkpoints distributed across the LMTC premises. Although this number is lower than the larger checkpoint counts recommended for broader standards-based summary reporting, the checkpoints were retained because of the limited campus-scale extent of the study area and the availability of clearly identifiable surveyed targets. To improve transparency of the assessment, the revised analysis includes not only summary statistics but also checkpoint-wise residual reporting for the independent checkpoints.

To summarise the magnitude of error, Root Mean Square Error (RMSE) and Mean Absolute Error (MAE) were computed. MAE represents the average magnitude of error without considering sign, whereas RMSE gives greater weight to larger residuals and is therefore more sensitive to larger deviations. Mean error was used to identify systematic bias in the products. A positive mean error indicates overestimation, while a negative mean error indicates underestimation. Standard deviation (SD) was used to describe the spread or consistency of the residuals. The 95% horizontal and vertical accuracy metrics were calculated to provide a confidence-based summary of product accuracy following NSSDA-style reporting (FGDC, 1998). All positional and vertical accuracy statistics are reported to three decimal places in meters for consistency and practical interpretability.

In addition to absolute positional assessment, a relative-geometry analysis was carried out to examine whether the without-GCP orthophoto was affected only by systematic displacement or also by scale-related geometric differences. This was assessed through pairwise distance comparison among the independent checkpoints and supplemented by selected object-based comparisons of digitized footprints on the with-GCP and without-GCP orthophotos.

Finally, the improvement achieved through GCP-based processing was expressed as a percentage difference between the with-GCP and without-GCP error values. This metric was used to quantify the practical benefit of field control for orthophoto, DSM, and DTM generation. The residuals and statistical measures were computed using Equations (1) to (12).

$$e_X = X_{model} - X_{survey} \quad (1)$$

$$e_Y = Y_{model} - Y_{survey} \quad (2)$$

$$e_Z = Z_{model} - Z_{survey} \quad (3)$$

$$e_H = \sqrt{e_X{}^2 + e_Y{}^2} \quad (4)$$

$$RMSE_X = \sqrt{\sum \frac{e_X{}^2}{n}} \quad (5)$$

$$RMSE_Y = \sqrt{\sum \frac{e_Y{}^2}{n}} \quad (6)$$

$$RMSE_Z = \sqrt{\sum \frac{e_Z{}^2}{n}} \quad (7)$$

$$RMSE_H = \sqrt{RMSE_X{}^2 + RMSE_Y{}^2} \quad (8)$$

$$MAE = \frac{\sum |e_i|}{n} \quad (9)$$

$$\text{Accuracy}_{H,95} = 1.7308 \times \text{RMSE}_H \quad (10)$$

$$\text{Accuracy}_{Z,95} = 1.96 \times \text{RMSE}_Z \quad (11)$$

$$\text{Improvement (\%)} = \left(\frac{\text{Error}_{without} - \text{Er}_{with}}{\text{Error}_{without}}\right) * 100\ \% \quad (12)$$

3.1 Orthophoto positional accuracy assessment

The orthophoto positional accuracy assessment based on eight independent checkpoints showed a clear improvement after the incorporation of Ground Control Points (GCPs). The checkpoint-wise residuals indicate that the with-GCP orthophoto produced only small planimetric residuals, whereas the without-GCP orthophoto showed substantially larger horizontal errors. These checkpoint-level results provide a clearer representation of the spatial distribution and consistency of positional error under both workflows.

Table 5. Checkpoint-wise residuals for orthophoto positional accuracy assessment under the with-GCP and without-GCP workflows.

CP	eX with-GCP (m)	eY with-GCP (m)	eH with-GCP (m)	eX without-GCP (m)	eY without-GCP (m)	eH without-GCP (m)
CP1	0.022	-0.039	0.045	-1.670	2.976	3.413
CP2	-0.042	0.039	0.057	-1.194	2.856	3.096
CP3	0.034	-0.033	0.047	-1.519	3.211	3.552
CP4	-0.070	-0.053	0.088	-1.400	2.337	2.725
CP5	0.026	-0.025	0.036	-1.107	2.194	2.458
CP6	-0.012	0.035	0.037	-1.867	3.572	4.031
CP7	0.036	-0.020	0.042	-2.618	3.564	4.422
CP8	0.088	0.001	0.088	-2.02	3.367	3.926

A visual comparison of the orthophotos generated under the two workflows is presented in Figure 3. Although the without-GCP orthophoto appears visually coherent, it does not align reliably with the surveyed checkpoint positions.

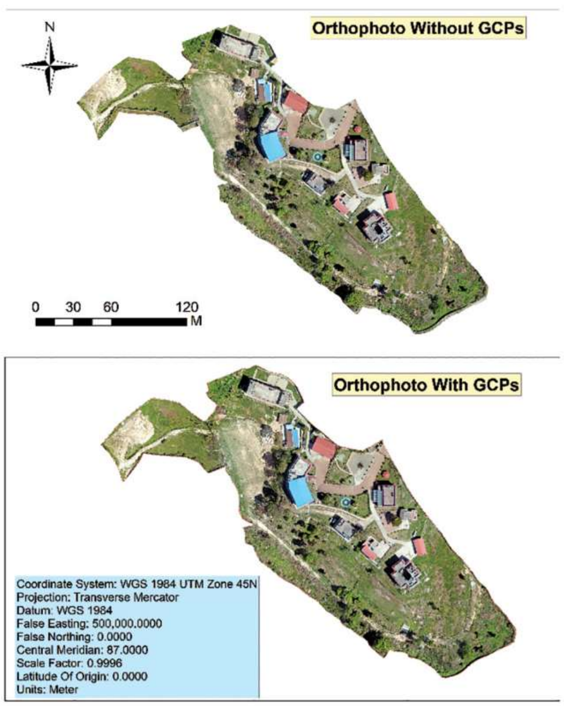

Figure 3. Orthophotos generated under the with-GCP and without-GCP workflows at the LMTC premises

The summary statistics further confirm the substantial improvement achieved through GCP-based processing. In the with-GCP workflow, the orthophoto produced RMSE values of 0.053 m in X and 0.034 m in Y, resulting in a combined horizontal $RMSE_H$ of 0.063 m and a 95% horizontal accuracy of 0.108 m. In contrast, the without-GCP orthophoto produced RMSE values of 1.731 m in X and 3.050 m in Y, yielding a combined $RMSE_H$ of 3.507 m and a 95% horizontal accuracy of 6.070 m. This corresponds to a horizontal RMSE improvement of 98.21% after the incorporation of GCPs.

Table 6. Summary statistics of orthophoto positional accuracy under the with-GCP and without-GCP workflows.

Statistic	With GCPs	Without GCPs
Mean Error X (m)	0.016	-1.669
Mean Error Y (m)	-0.012	3.010
MAE_X (m)	0.047	1.669
MAE_Y (m)	0.031	3.010
$RMSE_X$ (m)	0.053	1.731
$RMSE_Y$ (m)	0.034	3.050
$RMSE_H$ (m)	0.063	3.507
95% horizontal accuracy (m)	0.108	6.070
Median horizontal error (m)	0.052	3.471
SD horizontal error (m)	0.022	0.672
Min horizontal error (m)	0.036	2.458
Max horizontal error (m)	0.088	4.422

The error statistics show that the without-GCP orthophoto was affected not only by larger absolute error but also by systematic positional displacement. In the without-GCP workflow, the mean errors in X and Y were -1.669 m and 3.010 m, respectively, indicating a consistent westward and northward shift. In contrast, the with-GCP orthophoto showed near-zero mean residuals in both directions, indicating that the GCP-based adjustment effectively constrained the image block in map space. The largest horizontal error in the without-GCP case was observed at CP7, which lies near the outer part of the study area, suggesting weaker positional reliability toward the periphery of the uncontrolled block.

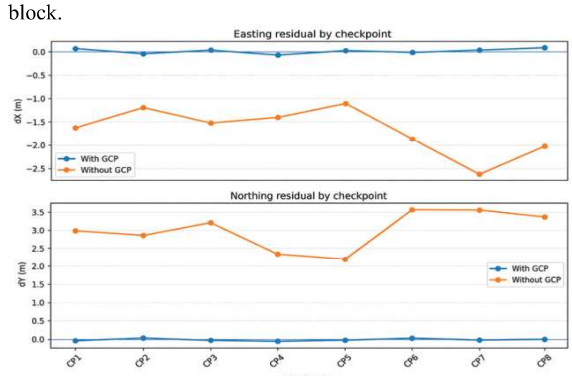

Figure 4. Easting and northing residuals of independent checkpoints under the with-GCP and without-GCP orthophoto workflows

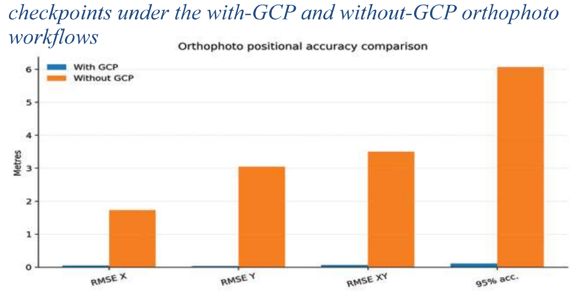

Figure 5. Comparison of key orthophoto positional-accuracy metrics under the with-GCP and without-GCP workflows

These results indicate that orthophotos generated without ground control may still possess weak absolute positional reliability. This finding is consistent with previous UAV photogrammetry studies reporting that products processed without sufficient external control can preserve general visual form while remaining unsuitable for precise planimetric measurement (Martínez-Carricondo et al., 2018; Sanz-Ablanedo et al., 2018; Szypuła, 2024).

3.2 Supplementary relative positional comparison of additional unsurveyed targets

In addition to the independent checkpoints, four extra pre-marked targets (EP1–EP4) visible in both orthophoto products were used for supplementary relative comparison. Because surveyed ground coordinates were not available for these targets, they were not included in the formal absolute accuracy assessment. However, they provide useful supporting evidence for evaluating relative positional differences between the with-GCP and without-GCP orthophotos.

The relative positional comparison of these additional targets is shown in Figure 6. The without-GCP orthophoto was displaced on average by -1.569 m in X and 3.254 m in Y relative to the with-GCP orthophoto, with a mean relative shift of 3.613 m. This displacement pattern is consistent with the westward and northward shift already identified from the independent checkpoint analysis. The relative positional differences for the four supplementary targets are summarised in Table 7, while the relative deviation pattern is further illustrated in Figure 7.

Figure 6. Relative positional comparison of additional points between the with-GCP and without-GCP orthophotos

Table 7. Relative positional differences of additional unsurveyed targets between the with-GCP and without-GCP orthophotos

Point ID	dX (m)	dY (m)	Relative shift (m)
EP1	-1.857	3.626	4.074
EP2	-1.397	2.929	3.245
EP3	-1.459	3.273	3.583
EP4	-1.562	3.190	3.552

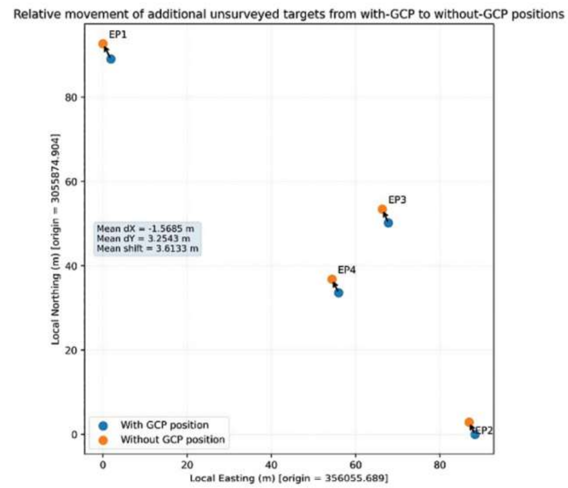

Figure 7. Relative deviation of additional points between the with-GCP and without-GCP orthophotos

The relative comparison based on these additional points supports the interpretation that the without-GCP orthophoto was systematically displaced in a broadly consistent manner across the study area. Although these targets cannot be used as independent absolute checkpoints, they provide useful supplementary evidence that the positional shift observed in the without-GCP orthophoto was not confined only to the formally surveyed checkpoints.

3.3 Relative geometry and scale-related differences in the orthophoto

To examine whether the without-GCP orthophoto was affected only by positional shift or also by relative geometric distortion, a pairwise distance analysis was carried out among the eight independent checkpoints. The results are presented in Table 8. The with-GCP orthophoto preserved checkpoint-pair distances very closely, whereas the without-GCP orthophoto showed consistently larger distances in nearly all checkpoint pairs. Scale factor was calculated as the ratio of orthophoto-derived checkpoint-pair distance to the corresponding surveyed checkpoint-pair distance, where values close to 1.000 indicate preservation of relative geometric scale.

Table 8. Pairwise distance comparison among the independent checkpoints under the survey, with-GCP, and without-GCP orthophoto datasets

Pair ID	Survey distance (m)	With-GCP distance (m)	Without-GCP distance (m)	Δdistance with-GCP (m)	Δdistance without-GCP (m)	Scale factor with-GCP	Scale factor without-GCP
CP1 - CP2	86.802	86.730	87.289	-0.072	0.487	0.999	1.006
CP1 - CP3	41.409	41.421	41.689	0.011	0.279	1.000	1.007
CP1 - CP4	102.618	102.568	103.277	-0.050	0.659	0.999	1.006
CP1 - CP5	133.979	133.973	134.921	-0.006	0.941	1.000	1.007
CP1 - CP6	76.807	76.888	77.434	0.081	0.627	1.001	1.008

CP1 - CP7	153.521	153.515	154.619	-0.006	1.098	1.000	1.007
CP1 - CP8	73.361	73.326	73.866	-0.034	0.505	0.999	1.007
CP2 - CP3	79.297	79.194	79.767	-0.104	0.470	0.999	1.006
CP2 - CP4	70.072	70.168	70.627	0.096	0.555	1.001	1.008
CP2 - CP5	80.858	80.932	81.525	0.074	0.667	1.001	1.008
CP2 - CP6	139.843	139.817	140.808	-0.027	0.964	1.000	1.007
CP2 - CP7	238.425	238.334	239.99	-0.091	1.564	1.000	1.007
CP2 - CP8	156.143	156.008	157.088	-0.135	0.945	0.999	1.006
CP3 - CP4	121.993	121.972	122.847	-0.021	0.854	1.000	1.007
CP3 - CP5	147.67	147.659	148.750	-0.011	1.081	1.000	1.007
CP3 - CP6	60.563	60.641	61.058	0.078	0.495	1.001	1.008
CP3 - CP7	165.357	165.356	166.491	0.000	1.135	1.000	1.007
CP3 - CP8	83.295	83.243	83.802	-0.052	0.507	0.999	1.006
CP4 - CP5	34.432	34.512	34.757	0.080	0.325	1.002	1.009
CP4 - CP6	176.685	176.728	177.978	0.043	1.293	1.000	1.007
CP4 - CP7	249.145	249.073	250.831	-0.072	1.686	1.000	1.007
CP4 - CP8	174.191	174.109	175.341	-0.081	1.150	0.999	1.007
CP5 - CP6	205.31	205.381	206.863	0.071	1.553	1.000	1.008
CP5 - CP7	282.957	282.951	284.958	-0.006	2.001	1.000	1.007
CP5 - CP8	206.67	206.638	208.116	-0.032	1.445	1.000	1.007
CP6 - CP7	116.556	116.516	117.301	-0.040	0.745	1.000	1.006
CP6 - CP8	47.572	47.522	47.824	-0.049	0.252	0.999	1.005
CP7 - CP8	82.619	82.665	83.244	0.047	0.626	1.001	1.008

The summary results of the pairwise distance analysis is presented in Table 9. The with-GCP orthophoto preserved checkpoint-pair distances very closely, with a mean absolute distance difference of 0.053 m, an RMSE of distance difference of 0.063 m, and a mean scale factor of 1.000. In contrast, the without-GCP orthophoto showed a mean absolute distance difference of 0.890 m, an RMSE of distance difference of 0.998 m, and a mean scale factor of 1.007. The minimum and maximum scale factors for the without-GCP orthophoto were 1.005 and 1.009, respectively. These results indicate that the no-control orthophoto was affected not only by systematic positional displacement but also by minor scale-related geometric differences.

Table 9. Summary of pairwise distance and scale-factor analysis among the independent checkpoints

Metric	With GCP	Without GCP
Mean absolute distance difference (m)	0.053	0.890
RMSE of distance difference (m)	0.063	0.998
Mean scale factor	1.000	1.007
Minimum scale factor	0.999	1.005
Maximum scale factor	1.002	1.009

A supplementary object-based comparison further supported this interpretation. Selected object footprints were digitized from the with-GCP and without-GCP orthophotos, and their areas and perimeters were compared (Table 10). For most selected objects, the without-GCP measurements were slightly larger than those derived from the with-GCP orthophoto. For example, the digitized area increased from 141.710 m² to 142.408 m² for the Administrative Building, from 341.586 m² to 343.101 m² for Boys Hostel, from 130.767 m² to 132.210 m² for the Canteen, and from 472.754 m² to 476.931 m² for the Executive Quarter. Similarly, perimeter values were generally greater in the without-GCP case. Although the Waiting Area showed a very small decrease in area, the overall pattern suggests that the without-GCP orthophoto was affected not only by systematic positional displacement but also by minor scale-related geometric differences.

Table 10. Supplementary object-based comparison of selected digitized features from the with-GCP and without-GCP orthophotos

Object name	Area with GCP (m²)	Area without GCP (m²)	Area difference (%)	Perimeter with GCP (m)	Perimeter without GCP (m)	Perimeter difference (%)
Administrative Building	141.710	142.408	0.49	49.487	49.663	0.360
Boys Hostel	341.586	343.101	0.440	100.523	100.860	0.330
Canteen	130.767	132.210	1.100	49.597	50.005	0.820
Control Point Buffer	10.405	10.607	1.940	11.478	11.600	1.060
Executive Quarter	472.754	476.931	0.880	87.746	87.983	0.270
Football Ground	1141.665	1156.786	1.320	139.885	140.836	0.680
Girls Hostel	268.249	270.610	0.880	73.884	74.123	0.320
Waiting Area	23.684	23.673	-0.040	17.952	18.063	0.620

The overlay of the selected digitized object footprints is shown in Figure 8, where the without-GCP outlines display both systematic displacement and slight enlargement relative to the with-GCP outlines.

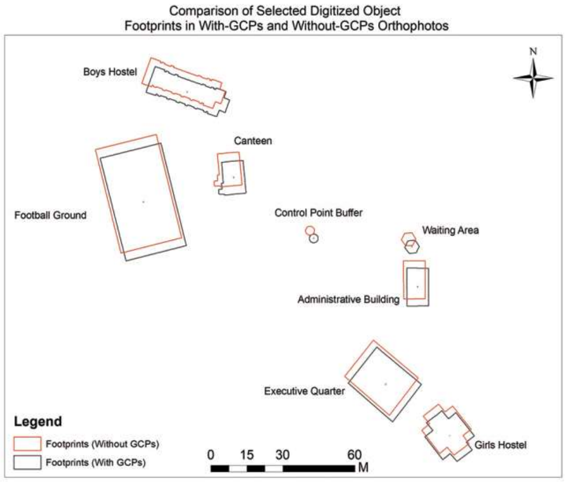

Figure 8. Overlay of selected object footprints digitized from the with-GCP and without-GCP orthophotos.

The without-GCP outlines show systematic positional displacement and slight geometric enlargement relative to the with-GCP outlines. Taken together, the pairwise distance analysis and the object-based comparison suggest that the without-GCP orthophoto was not affected only by translation-like shift. Rather, it also exhibited minor geometric expansion relative to the surveyed and with-GCP geometry. Because the object footprints were manually digitized and no independently surveyed rooftop dimensions were available, the object-based comparison is interpreted here as supplementary evidence of relative geometric consistency rather than as a formal absolute accuracy assessment. Nevertheless, both analyses consistently indicate that the no-control orthophoto retains reduced geometric fidelity even where the image appears visually coherent.

3.4 Vertical accuracy assessment at ground checkpoint locations

Because all vertical validation checkpoints used in this study were located on ground surfaces, the DSM and DTM assessments are presented here within a common vertical-accuracy framework. The DTM results directly represent ground-surface agreement, whereas the DSM results indicate elevation agreement at the same ground checkpoint locations only and do not constitute full validation of elevated surface features such as rooftops, vegetation canopies, or other above-ground objects.

3.4.1 DSM assessment at ground checkpoint locations

At the ground checkpoint locations, the DSM generated under the with-GCP workflow showed substantially better vertical agreement than the DSM generated without GCPs. As summarised in Table 11, the with-GCP DSM produced a mean vertical error of -0.053 m, a MAE of 0.110 m, and an $RMSE_Z$ of 0.131 m, corresponding to a 95% vertical accuracy of 0.256 m. In contrast, the without-GCP DSM showed a mean vertical error of 15.318 m, a MAE of 15.318 m, and an $RMSE_Z$ of 15.385 m, corresponding to a 95% vertical accuracy of 30.155 m. Thus, the incorporation of GCPs reduced DSM $RMSE_Z$ by 99.15%.

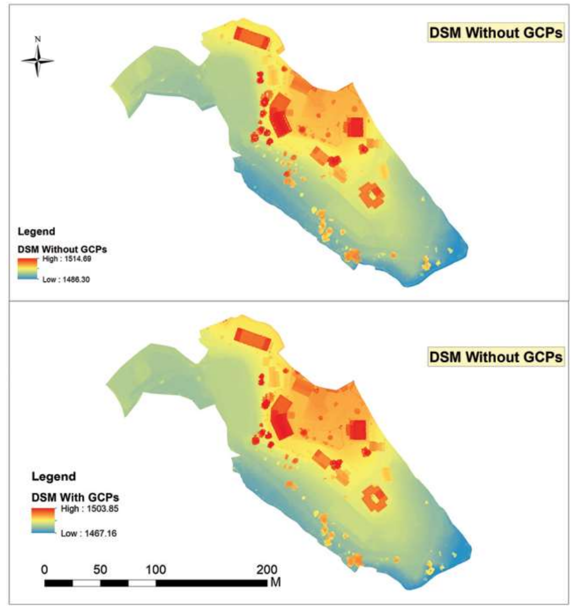

Figure 9. DSMs generated under the with-GCP and without-GCP workflows at the LMTC premises

Table 11. Summary statistics of DSM vertical agreement at ground checkpoint locations under the with-GCP and without-GCP workflows.

Statistic	With GCP	Without GCP
Mean Error $_Z$ (m)	-0.053	15.318
MAE $_Z$ (m)	0.110	15.318
RMSE $_Z$ (m)	0.131	15.385
95% vertical accuracy (m)	0.256	30.155
Median absolute error (m)	0.083	15.321
SD of error (m)	0.128	1.536
Min error (m)	-0.240	12.945
Max error (m)	0.083	17.686

The point-wise DSM height differences and the comparison of key DSM vertical-accuracy metrics are shown in Figures 10 and 11, respectively.

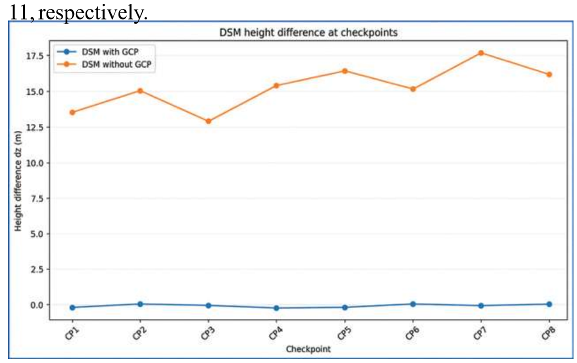

Figure 10. Point-wise DSM height differences between surveyed checkpoint elevations and DSM-derived elevations under the with-GCP and without-GCP workflows

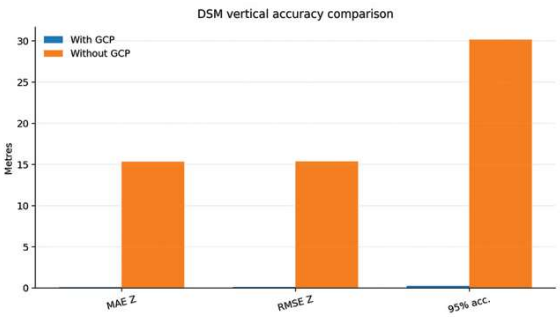

Figure 11. Comparison of key DSM vertical-accuracy metrics under the with-GCP and without-GCP workflows

3.4.2 DTM accuracy assessment

The DTM comparison showed a similarly strong effect of GCP incorporation. As shown in Table 12, the with-GCP DTM produced a mean vertical error of -0.070 m, a MAE of 0.121 m, and an $RMSE_Z$ of 0.143 m, corresponding to a 95% vertical accuracy of 0.280 m. In contrast, the without-GCP DTM produced a mean vertical error of 15.276 m, a MAE of 15.276 m, and an $RMSE_Z$ of 15.347 m, corresponding to a 95% vertical accuracy of 30.080 m. This represents a 99.07% improvement in $RMSE_Z$ after GCP incorporation.

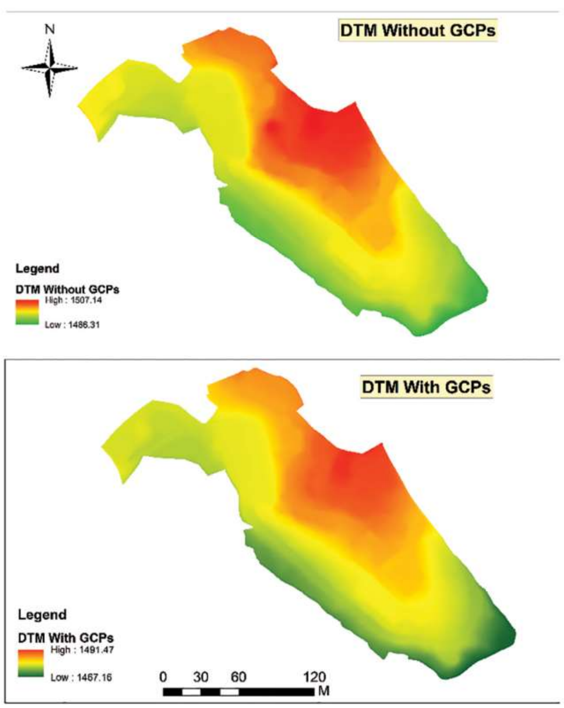

Figure 12. DTMs generated under the with-GCP and without-GCP workflows at the LMTC premises

Table 12. Summary statistics of DTM vertical agreement at ground checkpoint locations under the with-GCP and without-GCP workflows

Statistic	With GCP	Without GCP
Mean Error$_Z$ (m)	-0.070	15.276
MAE$_Z$ (m)	0.121	15.276
RMSE$_Z$ (m)	0.143	15.347
95% vertical accuracy (m)	0.280	30.080
Median absolute error (m)	0.078	15.316
SD of error (m)	0.133	1.575
Min error (m)	-0.252	12.947
Max error (m)	0.077	17.651

The point-wise DTM height differences and the comparison of key DTM vertical-accuracy metrics are presented in Figures 13 and 14, respectively.

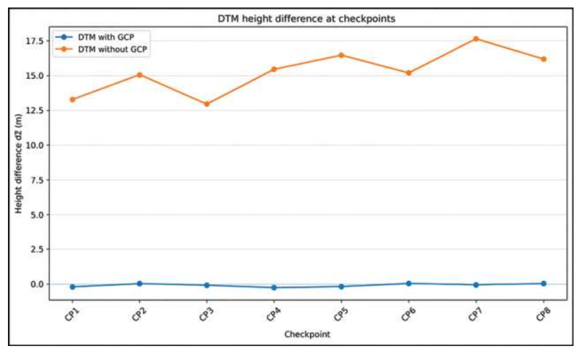

Figure 13. Point-wise DTM height differences between surveyed checkpoint elevations and DTM-derived elevations under the with-GCP and without-GCP workflows

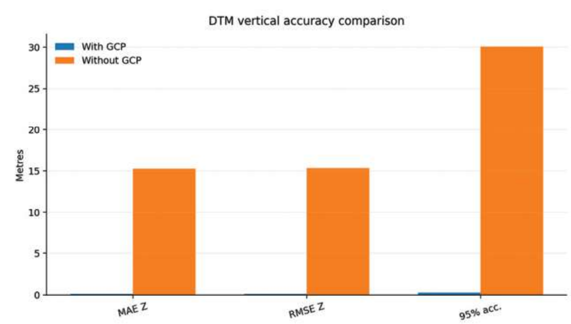

Figure 14. Comparison of key DTM vertical-accuracy metrics under the with-GCP and without-GCP workflows

An important feature of both elevation products is that the without-GCP case was affected mainly by a strong positive vertical offset. This is indicated by the large positive mean errors in both DSM and DTM, together with the comparatively smaller standard deviations of 1.536 m and 1.575 m, respectively. In other words, the no-control elevation products were not merely noisy; they were systematically displaced upward. This interpretation is also consistent with the visual comparison of the raster surfaces, in which the general surface pattern remains broadly similar while the absolute elevation level is markedly offset. Therefore, the main limitation of the without-GCP elevation products lies in absolute vertical positioning rather than complete loss of relative surface form.

The similarity between the DSM and DTM statistics is largely related to the ground-based location of all validation checkpoints. Because the checkpoints were located on ground surfaces, the DTM assessment is directly representative of bare-earth vertical agreement, whereas the DSM assessment reflects agreement at ground-visible locations only. For this reason, the DTM results provide the more direct interpretation of ground-surface vertical accuracy in the present study, while the DSM results should be understood more cautiously as ground-location vertical agreement rather than full-feature surface validation.

5. DISCUSSION

The results of this study show a clear and consistent improvement in product quality after the incorporation of Ground Control Points (GCPs). The with-GCP workflow produced centimetre-level horizontal accuracy in the orthophoto and decimetre-level vertical agreement in both the DSM and DTM, whereas the without-GCP workflow exhibited metre-level horizontal displacement and a strong positive vertical offset. These findings indicate that visually coherent UAV products generated without ground control may still possess weak absolute positional reliability and therefore cannot be assumed to be suitable for accurate mapping or measurement.

The orthophoto results show that the without-GCP product was affected by both systematic positional shift and minor relative geometric distortion. The checkpoint residuals presented in Table 5 and the summary statistics in Table 6 indicate a consistent westward and northward displacement in the without-GCP orthophoto. This interpretation is further supported by the supplementary relative comparison of the additional unsurveyed targets (Figure 6 and Table 7), which showed a similar displacement pattern. In addition, the pairwise checkpoint-distance analysis (Table 8 and Table 9) and the object-based footprint comparison (Table 10 and Figure 8) suggest that the no-control orthophoto was not affected only by translation-like shift, but also by small scale-related geometric differences. Although some internal geometric relationships may remain broadly preserved, the without-GCP orthophoto cannot be considered equivalent to the with-GCP product for applications requiring dependable absolute planimetric accuracy.

The vertical results lead to a similar conclusion. Both the DSM and DTM generated without GCPs retained broadly similar surface form, yet they were affected by strong positive elevation bias. This is evident from the large positive mean errors and RMSEZ values reported in Tables 11 and 12. At the same time, the relatively smaller spread of errors indicates that the without-GCP elevation products were not merely noisy, but systematically displaced upward. The observed pattern suggests that the primary limitation of the no-control elevation products lies in absolute elevation positioning rather than complete loss of relative surface form.

A further important point is that all vertical validation checkpoints used in this study were located on ground surfaces. Consequently, the DTM assessment directly represents bare-earth vertical agreement, whereas the DSM assessment reflects elevation agreement at ground checkpoint locations only and should not be interpreted as full validation of elevated surface features such as rooftops, vegetation canopies, or other above-ground objects. For this reason, the DTM results provide the more direct interpretation of ground-surface vertical accuracy in the present study, while the DSM results should be understood more cautiously.

The larger camera optimization difference observed in the without-GCP workflow also supports a more careful interpretation of the no-control results. The higher optimization difference indicates weaker geometric constraint in the uncontrolled image block, which suggests that the observed error should not be attributed to onboard image geolocation alone. Rather, the without-GCP results likely reflect the combined influence of weaker external control, onboard image geolocation uncertainty, image block geometry, and camera optimization instability. This is consistent with previous research showing that the number and spatial distribution of control points strongly influence the absolute positional and vertical quality of UAV-derived products (Martínez-Carricondo et al., 2018; Sanz-Ablanedo et al., 2018; Žabota et al., 2021; Szypuła, 2024).

Overall, the present study confirms that GCP-based processing remains essential for reliable campus-scale UAV mapping when the outputs are intended for measurement, planning, terrain representation, or other tasks requiring dependable absolute accuracy. Although the without-GCP workflow produced visually interpretable products, these outputs retained substantial positional and vertical bias and therefore are not suitable for applications where robust absolute accuracy is required.

5. CONCLUSION

This study evaluated the effect of Ground Control Points on the positional and vertical quality of UAV-derived orthophoto, DSM, and DTM products at the premises of the Land Management Training Center, Dhulikhel, Nepal, by processing the same UAV image block under with-GCP and without-GCP workflows. The results clearly demonstrate that GCP incorporation substantially improves both horizontal and vertical product reliability.

For the orthophoto, the with-GCP workflow achieved centimetre-level positional accuracy, while the without-GCP workflow showed metre-level horizontal displacement. The checkpoint residuals, the supplementary comparison of additional unsurveyed targets, the pairwise checkpoint-distance analysis, and the object-based footprint comparison consistently indicate that the no-control orthophoto was affected not only by systematic positional shift but also by minor scale-related geometric differences. Although the without-GCP orthophoto remained visually coherent, it did not provide dependable absolute positional accuracy for precise mapping and measurement.

For the elevation products, the with-GCP DSM and DTM showed much closer agreement with the surveyed checkpoint elevations, whereas the without-GCP products exhibited strong positive vertical bias. At the same time, the vertical error pattern suggests that the main weakness of the no-control products lies in absolute elevation positioning rather than complete loss of relative surface form. Because all validation checkpoints were located on ground surfaces, the DTM assessment provides the more direct interpretation of ground-surface vertical accuracy, while the DSM assessment should be understood as agreement at ground checkpoint locations only.

In summary, the findings demonstrate that GCP-based processing remains essential for reliable campus-scale UAV photogrammetry when the outputs are intended for measurement, engineering use, terrain representation, planning, or land-management applications requiring robust absolute accuracy. The without-GCP workflow may still retain limited relative geometric usefulness in some visually oriented or low-tolerance applications, but it cannot substitute for GCP-based processing where dependable absolute positional and vertical reliability are required.

A limitation of the present study is that the vertical validation checkpoints were confined to ground surfaces and no independently surveyed elevated-feature checkpoints were available. In addition, the study was conducted within a relatively small campus-scale area using a single processing software environment. Future studies could extend this work by testing denser and more widely distributed GCP networks, incorporating independently surveyed checkpoints on elevated features, and comparing the effects of alternative photogrammetric processing software and direct georeferencing strategies.

REFERENCES

FGDC. (1998). Geospatial positioning accuracy standards, Part 3: National standard for spatial data accuracy.

Gerke, M., & Przybilla, H.-J. (2016). Accuracy analysis of photogrammetric UAV image blocks: Influence of onboard RTK-GNSS and cross flight patterns. Photogrammetrie, Fernerkundung, Geoinformation, 2016(1), 17–30. https://doi.org/10.1127/pfg/2016/0284

Guth, P. L., Van Niekerk, A., Grohmann, C. H., Muller, J.-P., Hawker, L., Florinsky, I. V., Gesch, D., Reuter, H. I., Herrera-Cruz, V., Riazanoff, S., Lopez-Vazquez, C., Carabajal, C. C., Albinet, C., & Strobl, P. (2021). Digital elevation models: Terminology and definitions. Remote Sensing, 13(18), 3581. https://doi.org/10.3390/rs13183581

Kovanič, Ľ., Topitzer, B., Peťovský, P., Blišťan, P., Bindzárová, M. B., & Blišťanová, M. (2023). Review of photogrammetric and lidar applications of UAV. Applied Sciences, 13(11), 6732. https://doi.org/10.3390/app13116732

Manfreda, S., McCabe, M. F., Miller, P. E., Lucas, R., Madrigal, V. P., Mallinis, G., Ben Dor, E., Helman, D., Estes, L., Ciraolo, G., Mullerova, J., Tauro, F., de Lima, M. I., de Lima, J. L. M. P., Maltese, A., Frances, F., Caylor, K., Kohv, M., Perks, M., Ruiz-Perez, G., Su, Z., Vico, G., & Toth, B. (2018). On the use of unmanned aerial systems for environmental monitoring. Remote Sensing, 10(4), 641. https://doi.org/10.3390/rs10040641

Martínez-Carricondo, P., Agüera-Vega, F., Carvajal-Ramírez, F., Mesas-Carrascosa, F.-J., García-Ferrer, A., & Pérez-Porras, F.-J. (2018). Assessment of UAV-photogrammetric mapping accuracy based on variation of ground control points. International Journal of Applied Earth Observation and Geoinformation, 72, 1–10. https://doi.org/10.1016/j.jag.2018.05.015

Pix4D. (n.d.-a). Tie points in photogrammetry project (GCPs, CPs, MTPs, and ATPs).

Pix4D. (n.d.-b). Tie points (GCPs, MTPs, and CPs) – PIX4Dmatic.

Sanz-Ablanedo, E., Chandler, J. H., Rodríguez-Pérez, J. R., & Ordóñez, C. (2018). Accuracy of unmanned aerial vehicle (UAV) and SfM photogrammetry survey as a function of the number and location of ground control points used. Remote Sensing, 10(10), 1606. https://doi.org/10.3390/rs10101606

Szypuła, B. (2024). Accuracy of UAV-based DEMs without ground control points. GeoInformatica, 28, 1–28. https://doi.org/10.1007/s10707-023-00498-1

Žabota, B., Kokalj, Ž., Oštir, K., & Pehani, P. (2021). Accuracy assessment of UAV-photogrammetric-derived products using PPK and GCPs in challenging terrains: In search of optimized rockfall mapping. Remote Sensing, 13(19), 3812. https://doi.org/10.3390/rs13193812

AUTHOR INFORMATION

Name	:	**Bhuwan Singh Bisht**
Academic Qualification	:	MSc in Geoinformatics
Organization	:	Land Management Training Center
Current Designation	:	Instructor
Work Experience	:	7 years
Published Article	:	7